INSTITUTE OF PHYSICS PUBLISHING JOURNAL OF PHYSICS B: ATOMIC, MOLECULAR AND OPTICAL PHYSICS

J. Phys. B: At. Mol. Opt. Phys. **37** (2004) 147–163 PII: S0953-4075(04)66150-5

Dynamic stabilization of ground-state hydrogen in superintense circularly polarized laser pulses

M Boca[1], **H G Muller**[2] **and M Gavrila**[2]

[1] Department of Physics, University of Bucharest, Bucharest-Magurele MG11, 76900, Romania
[2] FOM Institute for Atomic and Molecular Physics, Amsterdam, 1098 SJ, The Netherlands

Received 11 July 2003
Published 9 December 2003
Online at stacks.iop.org/JPhysB/37/147 (DOI: 10.1088/0953-4075/37/1/009)

Abstract

We present a comprehensive calculation of 3D dynamic stabilization (DS) of ground-state hydrogen in superintense circularly polarized laser pulses. Three laser-pulse envelopes have been considered: Gaussian, sech, and Lorentzian. The ionization probability at the end of the pulse $P_{\rm ion}$ was calculated for a range of high frequencies ω ranging from 0.65 to 8 au, for peak fields up to about 60 au (depending on ω), and for full width at half maximum pulse lengths $\tau_{\rm p}$ extending from 0.25 to 100 cycles (depending on ω). This is a very accurate calculation, very much more time consuming than its linear polarization counterpart. For Gaussian and sech pulses we find prominent DS and substantial atomic survival under conditions where our nonrelativistic, dipole approximation calculation is expected to be valid. For Lorentzian pulses there is no DS in the range studied, and we explain the reasons. We find that the evolution of the atom is adiabatic and amenable to single-state Floquet theory, up to very large peak fields (several au), and down to very short pulses (few cycle, subfemtosecond). The general case of nonadiabatic pulses is interpreted in terms of the multistate Floquet theory. We compare the results for $P_{\rm ion}$ in the cases of circular and linear polarization and find a surprising resemblance, when represented as a function of the peak intensity. Our results indicate the possibility of observing DS experimentally with the VUV–FEL light sources that are now in test operation, or with the attosecond pulses obtained from high harmonic generation, in a state-of-the-art experiment, however.

(Some figures in this article are in colour only in the electronic version)

1. Introduction

Dynamic stabilization (DS) is a nonperturbative aspect of atomic ionization in superintense laser fields: by increasing the peak intensity of a laser pulse, while keeping the shape of its envelope fixed, the ionization probability of the atom does not grow to 1 (total ionization), but

starts decreasing (possibly in an oscillatory manner), or levels off at some value smaller than 1. Due to its counterintuitive nature, it has attracted considerable attention, and a vast theoretical effort went into its study in the decade elapsed since its discovery. (For an overview of atomic stabilization, see [1].) Computational difficulties have limited most theoretical studies to 1D models, and only a few have addressed the realistic problem of 3D hydrogen. For the ground state of the atom, detailed studies have also been discouraged by the realization that there appeared to be no prospect of detecting the phenomenon experimentally, as the conditions of observation required high-frequency lasers producing very short pulses, unavailable in the past. This has shifted the interest to DS of Rydberg states, for which the detection was eventually achieved [2, 3].

The experimental situation has improved dramatically in recent years, with the advent of superintense, ultrafast high-frequency radiation sources. Two types of sources have been conceived, and are being actively developed: VUV–FELs [4, 5], and attosecond pulses produced from high harmonic generation [6, 7]. Thus, the VUV–FEL at DESY is aimed at obtaining photon energies in excess of 200 eV, at intensities of 10^{19} W cm^{-2} and higher, in the form of pulses in the femtosecond range. Attosecond pulses are very short to start with; at a photon energy in the 80 eV range, a tight focusing could conceivably lead to some 10^{18} W cm^{-2} of intensity.

These advancements have prompted a comprehensive computation of DS for the ground state of H in order to reassess the observability of the phenomenon by Dondera *et al* [8, 9]. The case of linear polarization was considered, with pulses of both finite duration ($\cos^2$ envelope, [8]), and infinitely extended wings (Gaussian and sech envelopes, [9]). The ionization probability $P_{\rm ion}$ was mapped out over extended ranges of high frequencies, peak electric field amplitudes, and pulse durations $\tau_{\rm p}$. The conclusion was that detection of DS should be possible with the new light sources in a state-of-the-art experiment.

DS for circular polarization has received little attention in comparison to its linear counterpart. One of the reasons has undoubtedly been the much larger computational effort required for the circular case. As a consequence, there are no accurate 3D results on DS for ground-state H. Neither have experiments been performed.

Protopapas *et al* [10] and Patel *et al* [11], have considered DS for the ground state of a 2D model atom with a soft-core Coulomb potential of the form $V(\mathbf{r}) = -(a^2 + x^2 + y^2)^{-1/2}$, with a constant, at $\omega = 1$ au. DS was found to exist for arbitrary elliptic polarization, 'death valley' being deeper in the circular case than in the linear one. The properties of the time-dependent wavefunction obtained were studied for short pulses. A similar study for the same potential, and for circular polarization only, was carried out by Chism *et al* [12], at $\omega = 1.2$ au. The structure of the wavefunction was contrasted with the one in [11]. The calculation of the lifetimes resulted in excessively high values at larger field amplitudes (see section 3). Also Kwon *et al* [13] have studied DS from a 2D model atom and presented a few $P_{\rm ion}$ curves (their figure 1); the emphasis was on comparing classical and quantal behaviour.

A qualitative study of DS for 3D hydrogen was done by Choi and Chism [14]; the emphasis was on the properties of the atomic wavefunction, which manifests a peculiar rotating motion at high frequencies and intensities. Bauer and Ceccherini [15] have carried out a full 3D calculation for the ionization of the ground state of H using a time-dependent Schrödinger equation (TDSE) code. Although their emphasis was on two-colour stabilization, they derived results also for single-colour stabilization at $\omega = 1$ and 2, and variable field strength. Thus, they obtained stationary ionization rates at these frequencies by following the decay of the wavefunction in time for flat-top pulses (see section 3 below), as well as results for multiphoton ionization with finite duration pulses, and also studied the peculiar structure of the wavefunction (see also [14]). DS was briefly mentioned [15, figure 1].

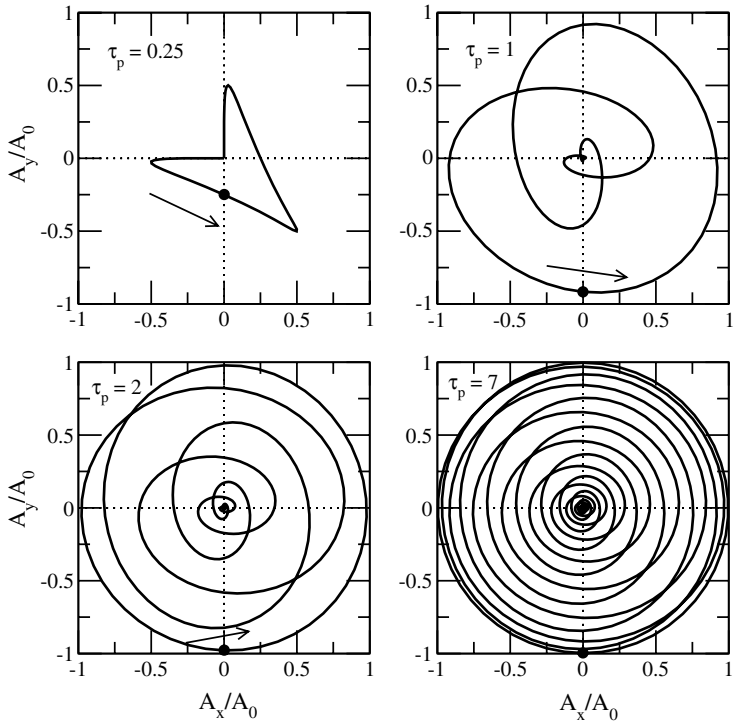

Figure 1. Trajectory of the tip of $\mathbf{A}(t)$, equation (1), for a Gaussian-pulse envelope, equation (2), at various widths τ_p, in cycles, as indicated. Time $t = 0$ is marked by a dot, and the sense of motion by an arrow.

We note also the early result by Gajda *et al* [16], for the excited $n = 2, l = 1, m = 0, \pm 1$, at $\omega = 0.25$ au, and 20 cycles pulses with a $\sin^2$ envelope. For the $m = 0, +1$ cases, DS was prominent, but much less for the $m = -1$ case, at least in the range of fields considered ($E_0 < 0.6$ au).

Quasistationary (adiabatic) stabilization (QS) has also been studied in a few cases for realistic 3D hydrogen and circular polarization. We recall that QS is the nonperturbative property of the atomic rate Γ to decrease (possibly in an oscillatory manner) beyond some critical value of E_0 (see [1, section 2]). In fact, it was the application of the high-frequency Floquet theory to the case of ground-state hydrogen and circular polarization that led to the discovery of QS by Pont and Gavrila [17]. Full Floquet calculations for the rate were carried out by Dörr *et al* [18] for the states 1s, 2s, at some high frequencies ($\omega > 0.5$ au), using the Sturmian approach (see also Potvliege [19]). Results for QS of the ground state and a comparison with other works were given by Bauer and Ceccherini at $\omega = 1$ and 2 in the aforementioned paper [15]. Zakrewski and Delande [20] have made a complex scaling calculation of Γ for the states $n = 2, l = 1, m = 0, \pm 1$, and frequency $\omega = 0.25$ au (a case considered earlier in the work of Gajda *et al* [16]). It was shown that DS had a surprisingly adiabatic character, even for very short pulses (see [1, section 3.2]).

In the present paper we want to explore the observability of DS for ground-state H, driven by a circularly polarized pulse. We shall consider pulses with Gaussian, sech, and Lorentzian field envelopes, at various peak values of the intensity, and cover the range of *high frequencies* ($\omega > 0.5$ au), at a variety of τ_p. We strive at obtaining comprehensive and highly

accurate results for $P_{\rm ion}$. The accuracy of our methods will be illustrated by comparing the quasienergies obtained with our TDSE code [21] to those obtained with the Sturmian Floquet code by Potvliege ([19], and private communication).

In the following, we discuss first the laser pulses we are using (section 2), then present the computation of $P_{\rm ion}$ (section 3), followed by the results (section 4) and their interpretation (section 5); we finally draw conclusions (section 6). We shall be using atomic units throughout, unless otherwise noted.

2. Laser pulses

A realistic 'circularly polarized laser pulse' is that emerging from a quarter-waveplate upon the incidence of a pulse of linearly polarized radiation. As a consequence the propagation along one of the optical axes is retarded by a quarter period with respect to the other. The vector potential of such a pulse is represented by

$$\mathbf{A}(t) = A_0[f(t)\sin\omega t\,\mathbf{e}_1 - f(t - T/4)\cos\omega t\,\mathbf{e}_2], \tag{1}$$

where $f(t)$ is the pulse envelope. We note that the need for taking a retarded pulse envelope $f(t - T/4)$ along one of the axes was ignored in earlier DS calculations [10–14, 16].

In the following, we shall be varying A_0 and ω, at fixed pulse envelopes $f(t)$. For the latter we shall use

$$\begin{aligned} f_{\rm G}(t) &= \exp[-(1.177t/\tau_{\rm p})^2], \\ f_{\rm sh}(t) &= \operatorname{sech}(1.763t/\tau_{\rm p}), \quad , \\ f_{\rm L}(t) &= [1 + (1.29t/\tau_{\rm p})^2]^{-1} \end{aligned} \tag{2}$$

where $\tau_{\rm p}$ represents the full width at half maximum (FWHM) for $\mathbf{A}^2$. These functions are very much alike in their central parts ($-\tau_{\rm p}/2 < t < +\tau_{\rm p}/2$), but differ substantially in the shape of their (infinitely extended) wings: the Gaussian pulse has rapidly decreasing wings, the sech pulse is an intermediate case, while the Lorentzian pulse has relatively slowly decreasing wings. The choice of these envelopes has an exploratory character, as those of the anticipated high-frequency light sources are not known.

The pulses equation (1), with the envelopes equation (2), satisfy for *arbitrary* $\tau_{\rm p}$ the conditions

$$\int_{-\infty}^{+\infty} \mathbf{A}(t)\,{\rm d}t = 0, \qquad \int_{-\infty}^{+\infty} \mathbf{E}(t)\,{\rm d}t = 0, \tag{3}$$

that have been shown to be necessary in order that the fields can represent physical pulses (see [1, section 3.1]). Under these conditions, the displacement and drift momentum *acquired* by a free classical electron at the end of the pulse are also zero: $(\delta\mathbf{r}) = 0$, $(\delta\mathbf{p}) = 0$. This classical situation corresponds to the maximum quantum mechanical overlap of the electron and atom wavefunctions at the end of the pulse, and should be optimal for the survival of the atom (see [1, sections 3.1 and 3.3]).

It is instructive to consider the trajectory of the tip of $\mathbf{A}(t)$ for pulses with various durations $\tau_{\rm p}$. This is given in figure 1, for a Gaussian-envelope pulse at $\tau_{\rm p} = 0.25; 1; 2; 7$. It is apparent that, for short pulses, there is little resemblance to the well known circular rotation pattern for a circularly polarized plane wave[3]. Moreover, it is obvious that, for short pulses, the distinction between 'circular' and 'elliptic' polarizations is meaningless.

[3] The trajectory of $\mathbf{A}(t)$ is symmetric with respect to the second diagonal of the reference axes A_x, A_y. Indeed, from equation (1) it follows that $A_x(t) = -A_y(-t + T/4)$, $A_y(t) = -A_x(-t + T/4)$. Consequently, to each point $[A_x(t), A_y(t)]$ of the trajectory, there corresponds a point $[-A_y(\tau), -A_x(\tau)]$, also on the trajectory, passed at $\tau = -t + T/4$, and hence the stated symmetry.

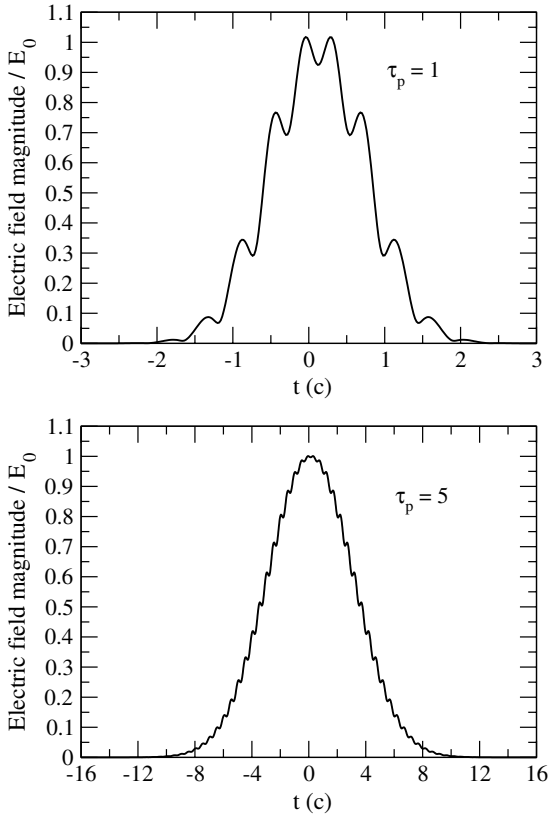

Figure 2. Time dependence of the electric field magnitude $|\mathbf{E}(t)|/E_0$ corresponding to $\mathbf{A}(t)$ of equation (1), where $E_0 = \omega A_0/c$, for a Gaussian pulse, at τ_p indicated (in cycles).

The electric field $\mathbf{E}(t)$ corresponding to equation (1) has a more complicated form. We represent the time dependence of its magnitude for a Gaussian pulse, and two pulse durations (a short one, and a longer one) in figure 2. To characterize the peak value of $|\mathbf{E}(t)|$, we introduce a nominal value, defined by the plane wave connection $E_0 = (\omega/c)A_0$. Figure 2 shows that E_0 gives a good description of the maximum of $|\mathbf{E}(t)|$, especially at larger τ_p. In the following we shall use interchangeably as variable either E_0 or I_0, the peak intensity corresponding to the nominal value E_0. We recall that the connection between E_0 and I_0 for a circularly polarized plane wave is $E_0 = (I_0/2)^{1/2}$, in contrast to the linear case, when we have $E_0 = I_0^{1/2}$.

3. Numerical procedures

We obtain $P_{\rm ion}$ by the standard procedure of calculating a sufficient number of survival probabilities in discrete n, l, m states at the end of the pulse, and taking the complement of their sum to 1. The TDSE is integrated in the velocity gauge using a highly efficient numerical code developed by one of us, that has been optimized in all possible ways [21]. In contrast to the linearly polarized case, considered in [8, 9], the running time here is much longer. This comes mainly from the fact that a much more extended spherical harmonics basis is needed: if the size of the basis is $L_{\rm max}+1$ in the linear case, it will be $(L_{\rm max}+1)(L_{\rm max}+2)/2$ in the circular case. Thus, for $E_0 \approx 5$ and $\omega = 2$, the difference in running time is of about a factor of 10.

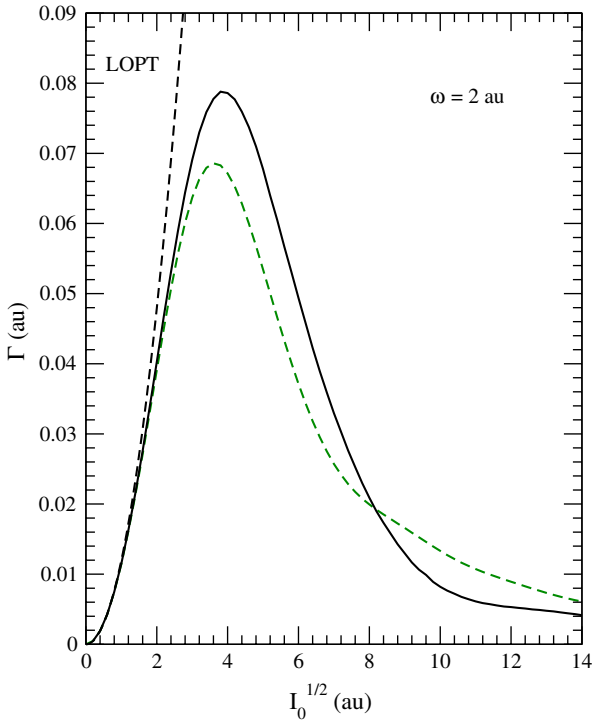

Figure 3. Solid curve: ionization rate Γ (in au) for ground-state H and circular polarization at $\omega = 2$ au, as a function of $I_0^{1/2}$ au, calculated from our TDSE program (see section 3). Dashed curve: Γ for linear polarization from the calculation by Dondera *et al* [8], figure 8. Also marked is Γ for the LOPT one-photon ionization rate.

Although the code has already been checked in low-frequency problems [22], we have undertaken a thorough testing of it also at high frequencies and for circular polarization. Thus, we have derived total ionization rates from our TDSE code and compared them, at small E_0, to rates from lowest-order perturbation theory (LOPT), and, at high nonperturbative E_0, to rates from Floquet theory. At small E_0, the agreement for Γ with the LOPT one-photon ionization rate (multiphoton contributions are negligible) was excellent; see also figure 3. We briefly describe the comparison for the nonperturbative regime.

Our TDSE rates were obtained by following in time the decay of the projection of the wavefunction Ψ on the field-free 1s state (specifically $|\langle 1s|\Psi\rangle|^2$) during the flat top of an adiabatically turned-on pulse. If the turn-on is sufficiently slow, Ψ can be represented at all times by just one Floquet state ('single-state Floquet theory'), and the decay during the flat top will be given by $e^{-\Gamma t}$, where Γ is the corresponding total ionization rate. In order to be able to extract an accurate Γ, a sufficiently long turn-on time must be chosen, to minimize the excitation of other Floquet states, as well as long flat tops for optimal fitting. (This becomes particularly critical at high E_0, because dE_0/dt has to be kept low during turn-on.) As the turn-on can never be infinitely slow, some discrete Floquet states will inevitably be excited, and this will perturb the exponential decay curve. Indeed, a close inspection of it reveals slight superimposed oscillations. The dominant ones are due to interference between the initial state i and lower excited states n; they occur at *atomic* transition frequencies $\mathrm{Re}(E_n - E_i)$, where $E_{n,i}$ are the corresponding quasienergies. This can be shown by spectral analysis of the

Table 1. Hydrogen quasienergies $E = W - \mathrm{i}(\Gamma/2)$ in a circularly polarized field (considered in section 2), at $\omega = 2$ au and various $\alpha_0 = E_0/\omega^2$, according to our TDSE calculation and the Floquet code of Potvliege [19]. The latter values bear the subscript P.

α_0	W	W_P	Γ	Γ_P
0.5	−0.445 97	−0.445 98	0.065 14	0.065 18
1	−0.341 38	−0.341 41	0.055 85	0.055 90
2	−0.253 35	−0.253 33	0.005 815	0.005 829
3	−0.201 76	−0.201 75	0.002 413	0.002 424
5	−0.143 72	—	0.000 4356	—
8	−0.101 03	—	0.000 1069	—

wavefunction during the flat top of the pulse. In fact, in our cases practically only one excited state was present beside the initial one. Then a two-state Floquet analysis of the situation allows the extraction of the initial state Γ with high accuracy. (A more detailed description of the procedure and the evaluation of errors will be given elsewhere.)

A TDSE code is capable of providing also the real part of the quasienergy, $E \equiv W - \mathrm{i}(\Gamma/2)$, if adiabatic pulses of the type described are used. For a wavepacket Ψ approximated by a single Floquet state, the projection on the unperturbed ground state can be written

$$\langle 1\mathrm{s}|\Psi\rangle \simeq \mathrm{e}^{-\mathrm{i}Wt}\mathrm{e}^{-(\Gamma/2)t}\Phi(t), \tag{4}$$

where $\Phi(t)$ is a periodic function. Thus, after each period $\langle 1\mathrm{s}|\Psi\rangle$ gets multiplied by $\mathrm{e}^{-\mathrm{i}W(2\pi/\omega)}\mathrm{e}^{-(\Gamma/2)(2\pi/\omega)}$. Knowledge of Γ yields W. To correct for possible nonadiabatic effects, the accuracy on W could be enhanced by a two-state Floquet approximation for Ψ. However, this is hardly needed, as for W the accuracy is much higher than that for Γ, to start with.

We present in table 1 our results for the quasienergies at $\omega = 2$ and a few values of α_0. The error analysis allows us to conclude that Γ is determined with an accuracy of better than 0.1%, and W to better than 0.05%. Also shown are results from the Floquet code of Potvliege [19]. The latter were obtained by just optimizing the available input parameters, (i.e., without trying to push the performance of the code to its limits). We found that the code became unstable beyond $\alpha_0 = 4$, so that $\alpha_0 = 3$ is the last value included in table 1. The agreement with our results is to better than 1% for Γ, and 0.1% for W.[4]

The curve for Γ at $\omega = 2$ is given in figure 3, where we have represented it as a function of $I_0^{1/2}$. This variable has been chosen so as to bring out the resemblance of the Γ curve for circular polarization and that for linear polarization, also shown in figure 3. The third curve shown is that of Γ from LOPT. Note that all three curves coincide at small intensity, as they should on theoretical grounds. Both Γ for circular and linear polarizations manifest QS: they attain a maximum, at about the same value $I_0^{1/2} \approx 4$, beyond which they decrease monotonically. In fact, the two curves have a rather similar shape, when represented in terms of $I_0^{1/2}$; when using as representation variables the two E_0, for circular and linear polarization, the two curves spread apart.

As another test of our code, we have calculated P_ion for the 2p, $m = 0, +1$ states of H, considered by Gajda *et al* [16, figure 1b]. We found agreement at the graphical level. Furthermore, our attention was attracted by the statement of Chism *et al* [12, see figure 1], that

[4] The asymptotic formula Γ_as of Pont and Gavrila for the circularly polarized case (see [1], equation (11) and figure 2) gives surprisingly good agreement with the values of Γ in table 1 even at low α_0. Thus, at $\alpha_0 = 1; 2; 3; 5; 8$, Γ_as gives 0.055 75; 0.006 969; 0.002 065; 0.000 4460; 0.000 1089, respectively. This new assessment should replace the critical comment made in [1], after equation (12).

in their 2D model calculations a 'dramatic increase of lifetime' occurred at $\omega = 1.2$ au, above $I \approx 10$ au, with lifetimes in the thousands of atomic units. This was totally out of line with the 3D hydrogen results of Dörr *et al* [18]. Hence, we have applied our 3D code to calculate the lifetimes of real H in the range considered, and have found indeed DS, but no dramatic increase of the lifetimes. Our results for the lifetimes are: 13.1 au at $\alpha_0 = 0.49$ ($F = 0.71$ in the notation of [12]); 8.95 au at $\alpha_0 = 0.98$ ($F = 1.42$); 57.9 au at $\alpha_0 = 1.96$ ($F = 2.82$); 130.3 at $\alpha_0 = 2.46$ ($F = 3.54$), whereas some 1800 au was found in this case in [12]; we are defining $\alpha_0 = E_0/\omega^2$ au.

In the determination of $P_{\rm ion}$ we calculate highly accurate transition probabilities to the individual n, l, m states. The accuracy on $P_{\rm ion}$, however, will depend on the number of states summed over. It is not difficult to achieve a final accuracy of 0.1% if desired.

We also mention that we have tested the effects on $P_{\rm ion}$ of ignoring the quarter-wave retardation of the envelope in the second term of equation (1), i.e., using $f(t)$ instead of $f(t - T/4)$. As most of the ionization occurs at the top of the pulse (where $f(t) \approx 1$), one might expect the effects to be negligible for long pulses such that $(T/4)/\tau_{\rm p} \ll 1$, and important in the opposite case. Indeed, by looking at $\omega = 2$, and $\tau_{\rm p} = 5$ cycles, we found no difference between the alternatives for Gaussian and sech pulses, but at $\tau_{\rm p} = 0.25$ the difference became 100% or more.

Our computation covers an extensive range of cases. The frequencies lie in the high-frequency (i.e., $\omega > 1$ Ryd) range $0.65 \leqslant \omega \leqslant 8$ au. At each ω, we have considered the pulse envelopes in equation (2), with FWHM pulse widths starting with $\tau_{\rm p} = 0.25$ cycles (a case of theoretical interest), and extending to values of $\tau_{\rm p}$ at which $P_{\rm ion}$ is not yet too close to 1. The peak electric field was taken in the range $0 < E_0 \lesssim 60$ au, with the maximum value depending on ω. This value was chosen such that the expected relativistic corrections would still be small. In this respect, we have used as guidance the 1D model calculations by Kylstra *et al* [23], which have shown that the corrections are negligible at $\omega = 2$ and $E_0 = 20$, and the fact that classical relativistic corrections scale as E_0/ω.

4. Results

We show in figures 4–7 some of our results for $P_{\rm ion}$ represented as function of $I_0^{1/2}$, at fixed ω, for the envelopes G, sech, L, at different $\tau_{\rm p}$. We signal the following features.

In nearly all cases, at given ω, $\tau_{\rm p}$, $I_0^{1/2}$, we see that

$$P_{\rm ion}^{\rm G} < P_{\rm ion}^{\rm sech} < P_{\rm ion}^{\rm L}. \tag{5}$$

This can be explained by the fact that, under the circumstances, the field amplitudes, while more or less the same in the central parts for all envelopes, are larger in the wings as one proceeds along the sequence G, sech, L, thus leading to more ionization.

At small $I_0^{1/2}$, for all ω, $\tau_{\rm p}$, the curves of $P_{\rm ion}^{\rm G}$, $P_{\rm ion}^{\rm sech}$, $P_{\rm ion}^{\rm L}$, are closely bunched together, starting from zero and rising steeply. This is the LOPT regime, dominated by one photon ionization. The rapid growth of $P_{\rm ion}$ subsides at some value of $I_0^{1/2}$ (depending on ω, $\tau_{\rm p}$), and is replaced by the nonperturbative regime, characterized either by a decrease, a plateau, or a slow increase with $I_0^{1/2}$.

The decrease or plateau behaviour of $P_{\rm ion}$ with respect to $I_0^{1/2} = E_0/\omega$ represents, according to our definition of section 1 (see also [1, section 3]), *dynamic stabilization*. DS occurs for the Gaussian and sech envelopes in all cases shown (for $\tau_{\rm p} < 1$ and $\omega = 4, 8$, the growth of $P_{\rm ion}$ has not been completed over the range of $I_0^{1/2}$ shown). The values of $P_{\rm ion}$ become larger when increasing $\tau_{\rm p}$ at fixed ω. If $\tau_{\rm p}$ is long enough, $P_{\rm ion}$ gets to be

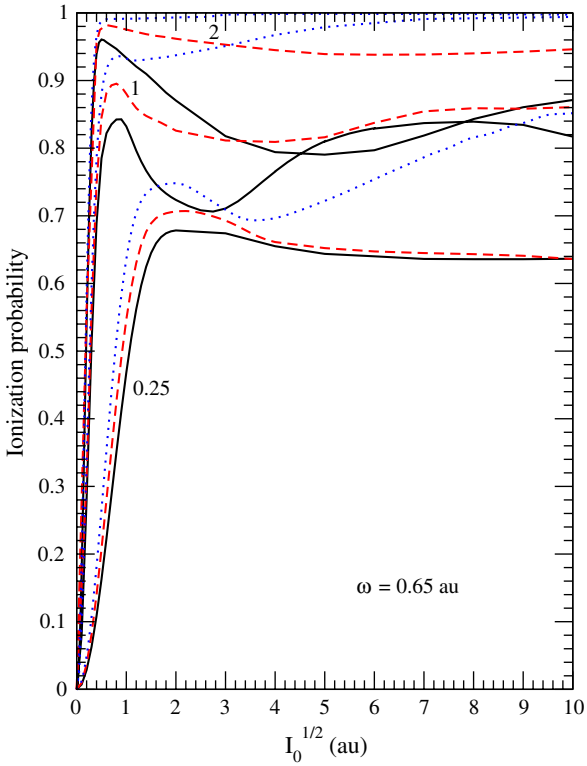

Figure 4. Ionization probability $P_{\rm ion}$ of ground-state H exposed to the pulses in equation (1), with $\omega = 0.65$ au, and the envelopes in equation (2), at various pulse widths $\tau_{\rm p}$ (in cycles), as a function of $I_0^{1/2} = \sqrt{2}E_0$ (in au). Solid curves: Gaussian pulses; dashed curves: sech pulses; dotted curves: Lorentzian pulses. The value of $\tau_{\rm p}$ is specified next to the $P_{\rm ion}$ curves coalescent at small $I_0^{1/2}$.

indistinguishable from 1. For example, for the Gaussian envelope, one may consider the curves for $\tau_{\rm p} = 5, 25, 100$ cycles, at $\omega = 2, 4, 8$, respectively, to be still significantly different from 1, so that DS be detectable. The corresponding values in femtoseconds are: $\tau_{\rm p} = 0.38, 0.95, 1.90$ fs. The FWHM pulse durations required to observe DS are thus quite short, of the order of the femtosecond, or less.

It is apparent from the figures that there is *no DS for Lorentzian envelopes* in the range of $I_0^{1/2}$ shown (except for $\omega = 2$ and $\tau_{\rm p} = 0.25$). This fact was first signalled for Rydberg states by Piraux and Potvliege [24]. The explanation will be given below. It should be noted, however, that the Lorentzian envelope is rather unlikely to occur in practice.

For a given envelope, and at fixed $\tau_{\rm p}$, $I_0^{1/2}$, we note that $P_{\rm ion}$ is smaller, the higher ω is. This is specific to the high frequencies we are considering. We note that the case of $\omega = 0.65$ is only marginally a high-frequency case. This manifests itself in the fact that (in the range of $I_0^{1/2}$ considered), although $P_{\rm ion}$ undergoes significant DS for extremely short $\tau_{\rm p}$, for longer $\tau_{\rm p}$ it becomes practically 1 (not shown in figure 4).

One may inquire about the behaviour of $P_{\rm ion}$ beyond the range of peak fields we have explored. Figures 5–7 suggest that $P_{\rm ion}$ starts rising at the end of the range even for the Gaussian and sech pulses, i.e., that the DS regime would be followed by a *'destabilization regime'*. This, indeed, was shown to be the case for the ground-state H and linear polarization,

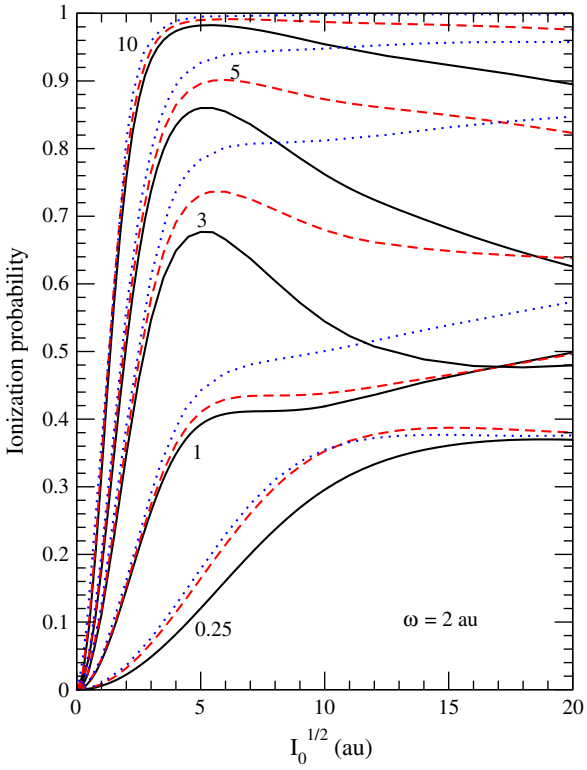

Figure 5. The same as for figure 4, except that $\omega = 2$ au.

with $\cos^2$ envelopes at $\omega = 8$, in [8, figure 7]. The calculation was carried out there up to $E_0 = 3000$, and it revealed that the DS regime is followed by a destabilization regime, and, at still higher E_0, possibly by another plateau-like DS regime. In this respect it is interesting to mention the rigorous mathematical result of Fring *et al* [25, theorem 3], which states that, at fixed pulse envelope of *finite* duration satisfying the conditions (3), for $E_0 \to \infty$ we have $\lim P_{\rm ion} < 1$. The findings in [8, figure 7] indicate that this would happen only at extremely high E_0. The present pulses, however, have infinite duration, and it is an open question to what extent the theorem could be generalized to this case. Obviously, the discussion of the $E_0 \to \infty$ limit is of academic interest within NR theory, since at very large fields, relativistic effects become essential.

5. Discussion

Let us first focus on our results for *adiabatic pulses*, i.e., for which $\mathrm{d}E_0(t)/\mathrm{d}t$ is sufficiently small throughout the pulse. This case can be interpreted in terms of *single-state Floquet theory*, see [1, section 3.2]. The ionization probability at the end of the pulse can then be written

$$P_{\rm ion}^{\rm (ad)} = 1 - \exp\left[-\int_{-\infty}^{+\infty} \Gamma[E_0(t)]\,\mathrm{d}t\right]. \tag{6}$$

Conversely, the fact that the dynamically calculated $P_{\rm ion}$ coincides with $P_{\rm ion}^{\rm (ad)}$ is an indication that the evolution is adiabatic. To make the comparison, the value of Γ is needed over the

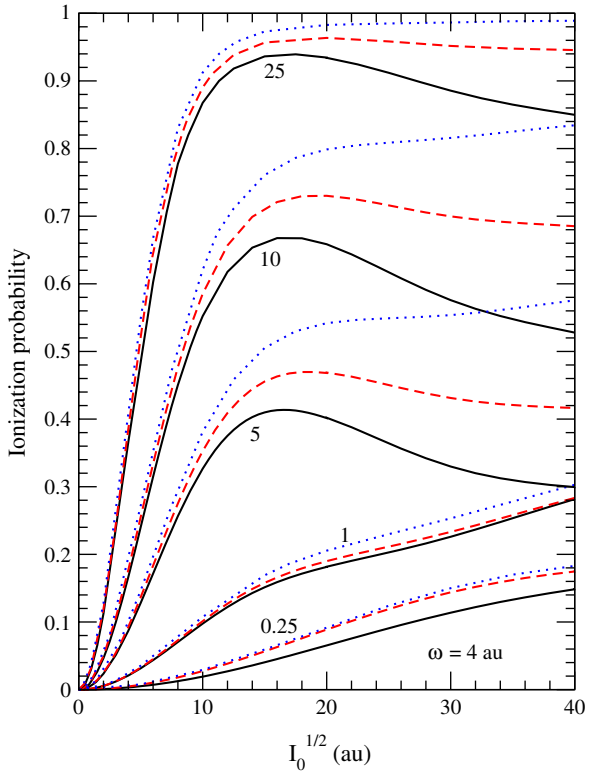

Figure 6. The same as for figure 4, except that $\omega = 4$ au.

whole range of variation of $E_0(t)$. We have described the calculation of Γ by two methods in section 3, and the results at $\omega = 2$ were given in figure 3.

The comparison of P_{ion} and $P_{\text{ion}}^{(\text{ad})}$ at this frequency in terms of $I_0^{1/2}$ is shown in figure 8 for the envelopes considered. The agreement extends to surprisingly high values of I_0 for all three envelopes, even for such short pulses as $\tau_{\text{p}} = 5$. This was first signalled in the study by Zakrewski and Delande [20] of the excited states $n = 2$. The deviation of P_{ion} and $P_{\text{ion}}^{(\text{ad})}$ is a measure of the magnitude of the excitation to higher Floquet states ('shake-up'). Their close agreement for ground-state H is a consequence of the relatively large energy gap between the ground and the first excited state energies, that inhibits shake-up. The agreement is obviously improved as τ_{p} is increased at given ω.

Note that the maxima of P_{ion} in figures 5–7 occur at intensities that correspond approximately to the maxima of Γ for the ω considered (minima of the lifetimes, 'death valleys'), as calculated by Pont and Gavrila (for example, see [1], figure 2). This is another manifestation of the applicability of equation (6).

Our results for arbitrary pulses can be interpreted in terms of the *multistate Floquet theory* (MSFT), as was done for the linearly polarized case [8], [1, section 3.2]. This consists of analysing the evolution of the physical wavepacket in terms of superpositions of Floquet states:

$$\Psi(\mathbf{r}, t) \propto \mathsf{S}_\nu C_\nu(E_0)\psi^{(\nu)}(\mathbf{r}, t; E_0, \omega), \tag{7}$$

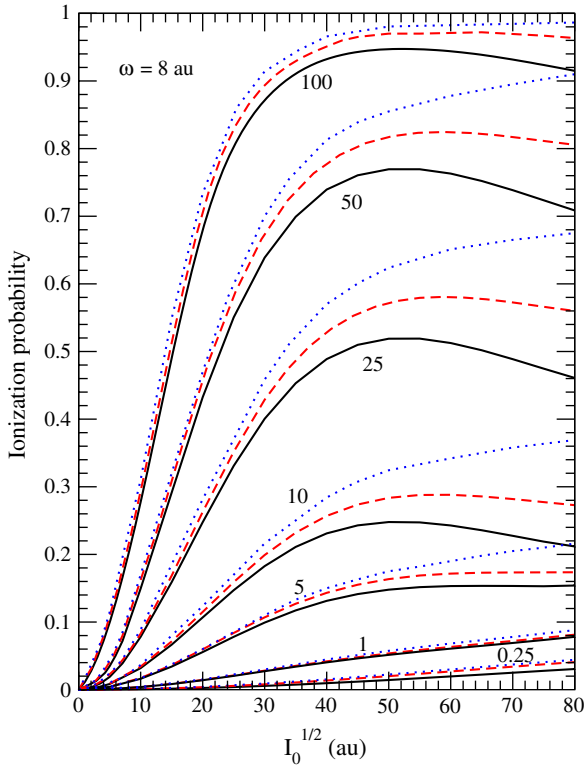

Figure 7. The same as for figure 4, except that $\omega = 8$ au.

where $\psi^{(\nu)}(\mathbf{r}, t; E_0, \omega)$ are the individual Floquet states, and E_0 is the field amplitude. The summation $\mathbf{S}_\nu$ extends over discrete quasienergy states, but should include also an integration over continuum states along an adequate contour in the complex energy plane. In a constant amplitude field E_0, the coefficients $C_\nu(E_0)$ are constant; in a variable-amplitude field, they are time dependent, and $\psi^{(\nu)}(\mathbf{r}, t; E_0, \omega)$ acquires an extra time dependence due to $E_0(t)$.

At low E_0 the evolution of the system is, in most cases, adiabatic, and in equation (7) we can retain only a single Floquet state, that corresponding to the initial state. We are then in the realm of single-state Floquet theory considered previously. However, by keeping the pulse envelope fixed and increasing E_0 (or $I_0^{1/2}$), as we have done in figures 4–8, the adiabaticity is gradually lost ($\mathrm{d}E_0(t)/\mathrm{d}t$ becomes too large at some time during the pulse), and P_{ion} starts deviating from $P_{\mathrm{ion}}^{(\mathrm{ad})}$. This means that several Floquet states need to be included in the expansion equation (7). As a consequence, at the end of the pulse the system will have population in excited field-free states n, l associated with these Floquet states. Because ionization from higher Floquet states has reduced rates, shake-up means smaller P_{ion}, and hence shake-up should help DS. This is confirmed by the fact that in figure 8, systematically $P_{\mathrm{ion}} \leqslant P_{\mathrm{ion}}^{(\mathrm{ad})}$. However, a *change in the physical origin of DS* has set in: from adiabatic (QS related) to nonadiabatic (shake-up related).

Beyond some critical value E_0, population will also be transferred directly into the continuum during the turn-on (extremely large $\mathrm{d}E_0(t)/\mathrm{d}t$). Consequently, the expansion (3) will develop contributions from continuum Floquet states. Even in these states, the system is subject to multiphoton ('free–free') transitions, but the yields are smaller the larger the

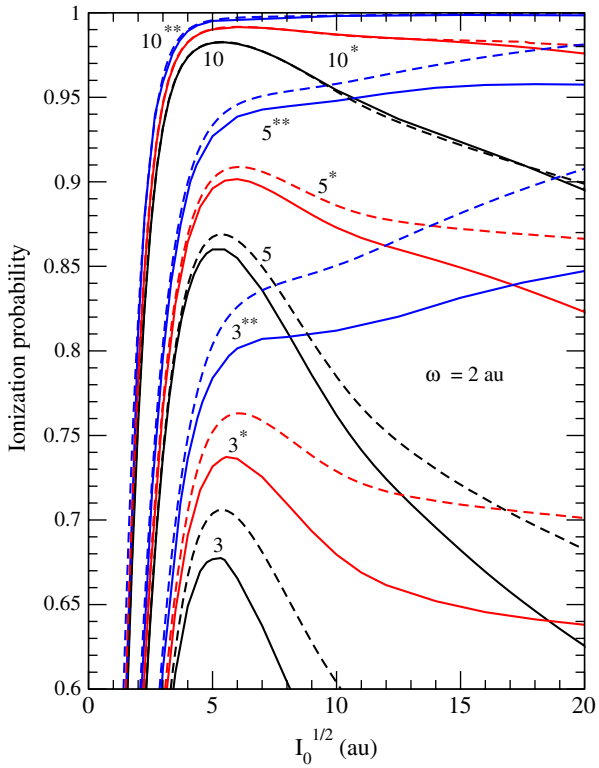

Figure 8. Comparison at $\omega = 2$ au of $I_0^{1/2}$- dependence of the ionization probability of ground-state H exposed to the pulses in equation (1). Solid curves: TDSE computation; dashed curves: adiabatic approximation equation (6). The values of τ_p (in cycles) are given next to pairs of such curves. The τ_p for Gaussian pulses carry no asterisk, for sech pulses they carry one asterisk, and for Lorentzian pulses, two asterisks.

electron energy is, so that high in the continuum, the electron oscillates practically like a free particle, with negligible influence from the nucleus and negligible loss of energy. During the turn-off, the atom undergoes another shock, which may allow it to recapture part of this freely oscillating population, but some of it will end up in the continuum of the unperturbed atom and will disperse. This effect we shall denote as 'shake-off'. We are dealing here with a *change in the physical nature of the ionization*: from *multiphoton ionization*, involving absorption of photons, that can be described in terms of several discrete Floquet states and gives rise to well defined lines in the EPI/ATI spectrum, to *shake-off ionization*, caused by the shock of the field amplitude, that cannot be described in terms of discrete energy photons, and gives a continuum background in the EPI/ATI spectrum (the issue will be elaborated on elsewhere).

We shall now address the issue of the difference in DS for the various envelopes in figures 4–7. For this we shall rely on equation (6), as it gives in all cases an adequate qualitative result. We want to show that the difference stems from the pedestal of the envelopes. We split the integral J appearing in equation (6) under the exponential (representing the convolution of $\Gamma(E_0)$ with the pulse envelope $E_0(t)$), in two parts: J_1, the contribution of the central part of the envelope, and J_2, that of the pedestal: $J = J_1 + J_2$. We define the pedestal as being the part of the envelope for which $|t| > \tau_p$. Thus, equation (6) becomes

$$P_{\text{ion}}^{(\text{ad})} = 1 - \exp(-J_1)\exp(-J_2). \tag{8}$$

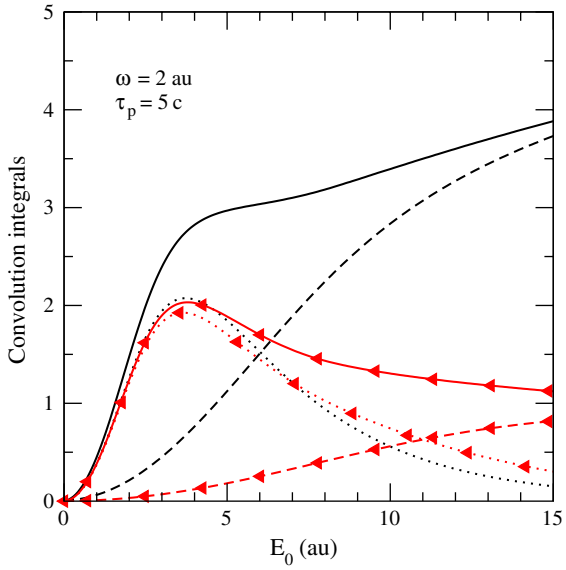

Figure 9. Convolution integrals J_1, J_2, J, as defined in text, for Gaussian and Lorentzian pulses with $\omega = 2$ and $\tau_p = 5$ cycles; the Gaussian curves are distinguished by triangles. J_1 (centre of pulse contributions): dotted curves; J_2 (pedestal of pulse contributions): dashed curves; $J = J_1 + J_2$: solid curves.

In figure 9 we consider the values of J_1, J_2, J for the Gaussian and Lorentzian pulses, at $\omega = 2$ and $\tau_p = 5$. The figure shows that for all E_0 the contributions of the central parts J_1 are about equal; this was to be expected, as the central parts of the envelopes are nearly the same. Moreover, these contributions are decreasing functions at large E_0. This is because, beyond a certain E_0, the central part of the envelope is pushed progressively into the range in which Γ decreases (see figure 3). On the other hand, the pedestal contributions J_2 differ greatly, the one for the Lorentzian growing much faster with E_0. This is because, although at growing E_0, the peak of Γ ('death valley') is convoluted with increasingly distant points of the envelope, this being nonvanishing, it keeps adding up to the integral in equation (6). The wings of the Lorentzian being much broader, the build-up is much larger than for the Gaussian. Since J_1 is about the same in both cases, but J_2 is much larger for the Lorentzian, according to equation (8), $P_{\rm ion}^{\rm (ad)}$ will be considerably larger for the Lorentzian. Moreover, due to the actual numerical values of the exponentials in equation (8), $P_{\rm ion}^{\rm (ad)}$ turns out to be decreasing with E_0 for the Gaussian, and increasing for the Lorentzian (no DS).

It is natural to compare our DS results for circular polarization with those obtained by Dondera *et al* for linear polarization [9]. We show the comparison for $P_{\rm ion}$ at $\omega = 2$ and 4 in figures 10 and 11, respectively, for sech pulses at different τ_p. The resemblance of the corresponding curves, not only in terms of shape, but also actual values is striking. (The same happens for Gaussian pulses.) This is rather remarkable, because after all, we are dealing with different physical situations, leading to different kinds of distortion of the atom in the nonperturbative regime. We propose to explain the resemblance by two facts. One is the pervasive validity of the adiabatic approximation to $P_{\rm ion}$, equation (6), even for short pulses; see figure 8. The other is the overall resemblance of Γ for the two cases, illustrated in figure 3. Note that the resemblance of $P_{\rm ion}$ is brought out by representing them in terms of $I_0^{1/2}$; had we used the variables E_0 corresponding to circular and linear polarization instead, the two

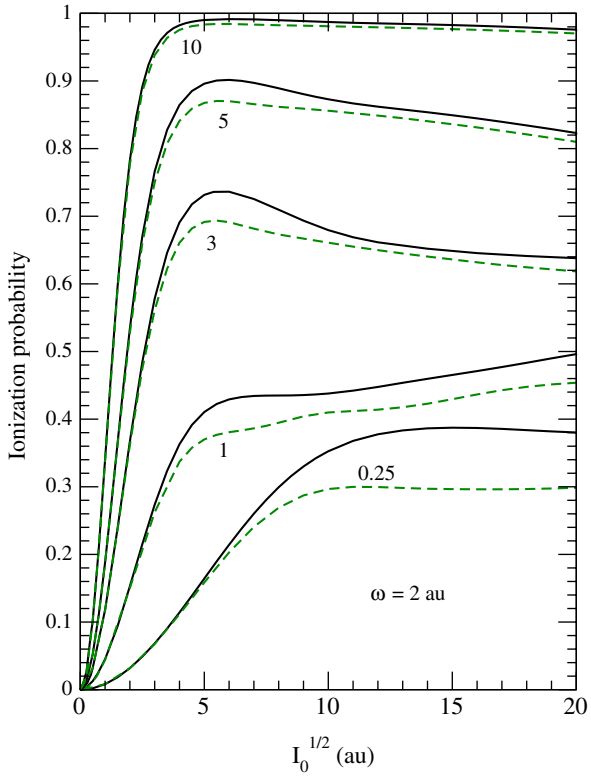

Figure 10. Comparison of P_{ion} for circular and linear polarizations; sech pulses are considered with $\omega = 2$ au and the indicated widths τ_{p}. Solid curves: circular polarization; dashed curves: linear polarization.

curves would have spread apart. One may argue that the representation in terms of I_0 is more physical, as I_0 is an observable quantity.

Finally, with our numerical results at hand, we consider the *possibility of experimental detection of DS* with VUV–FEL radiation or attosecond pulses from high-harmonic generation. In both cases, the presently available frequencies are satisfactorily high. So are the intensities. The pulse length, however, is still a problem at the DESY machine, as the targeted value for the near future is only some 30–50 fs, whereas, as mentioned above, durations of a few femtoseconds are needed for DS. The gap could be bridged in principle by optical seeding with suitably chosen XUV radiation, allowing for chirped-pulse amplification. Obviously, attosecond pulses offer in this respect a very favourable starting point. The perennial difficulty of having a large intensity distribution in the laser focus, which would completely blur DS, could be countered by preparing the atoms in a sufficiently small region of the focus, as was done in the stabilization experiment on Rydberg atoms [2, 3].

6. Conclusions

The calculation of the ionization probability of ground-state H with circularly polarized pulses shows substantial DS at high frequencies for Gaussian and sech envelopes, over an extended range of field amplitudes, at which our nonrelativistic calculation is expected to be valid.

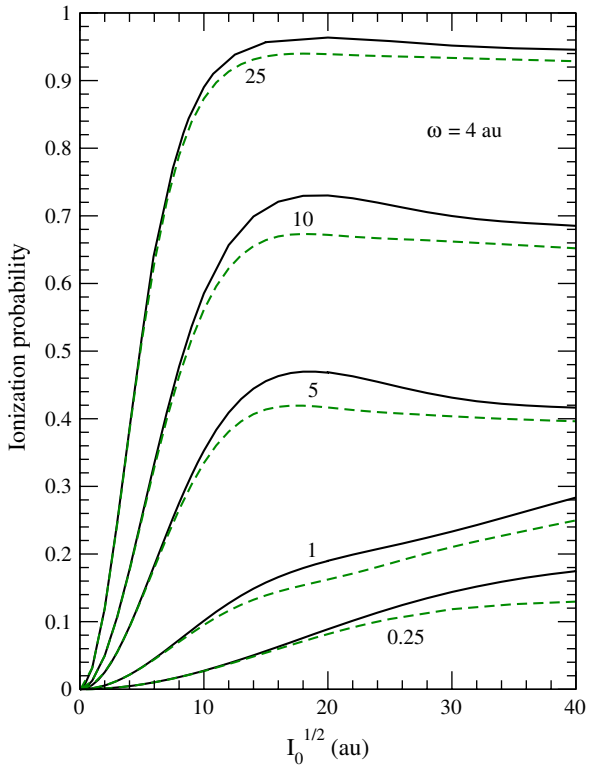

Figure 11. The same as for figure 10, except that $\omega = 4$ au.

In contrast, for Lorentz pulses we find no DS in the same field range. This is traced back to the very broad pedestal of these pulses. Moreover, the evolution of the atom is remarkably adiabatic up to large peak fields, and down to very short pulses. The results for the Gaussian and sech envelopes are similar to those obtained by Dondera *et al* [9] for linearly polarized pulses and similar envelopes, if $P_{\rm ion}$ is represented in terms of the peak intensity I_0.

Our high-accuracy TDSE numerical code gives quasienergies in excellent agreement with the Floquet values of Potvliege [19]. This emphasizes the fact that, after many years of qualitative results, laser–atom interaction theory is now capable of producing consistently accurate 3D predictions.

The calculations indicate the possibility of observing DS experimentally with the new FEL–VUV light sources, or with attosecond pulses generated from high-harmonic generation. However, the experiment should be state-of-the-art, at the frontier of present capabilities.

Acknowledgments

The authors thank R M Potvliege for useful comments regarding his code, and M Dondera for useful numerical input. They acknowledge the support of the following organizations: CNCSIS, the Romanian Scientific Research Council for Higher Education, grant 365/2002 (MB); FOM, which is a division of the Netherlands Organization for Advancement of Science, via its research programme (HGM); IR Foundation (MG).

References

[1] Gavrila M 2002 *J. Phys. B: At. Mol. Opt. Phys.* **35** R147
[2] de Boer M P, Hoogenraad J H, Vrijen R B, Constantinescu R C, Noordam L D and Muller H G 1993 *Phys. Rev. Lett.* **71** 3263
de Boer M P, Hoogenraad J H, Vrijen R B, Constantinescu R C, Noordam L D and Muller H G 1994 *Phys. Rev.* A **50** 4085
[3] van Druten N J, Constantinescu R C, Schins J M, Nieuwenhuize H and Muller H G 1997 *Phys. Rev.* A **55** 622
[4] Andruszkow J *et al* 2000 *Phys. Rev. Lett.* **85** 3825
[5] Ayvazian V *et al* 2002 *Phys. Rev. Lett.* **88** 104802
[6] Paul P M *et al* 2001 *Science* **292** 1689
[7] Hentschel M *et al* 2001 *Nature* **414** 509
[8] Dondera M, Muller H G and Gavrila M 2002 *Laser Phys.* **12** 415
[9] Dondera M, Muller H G and Gavrila M 2002 *Phys. Rev.* A **65** 031405(R)
[10] Protopapas M, Lappas D G and Knight P L 1997 *Phys. Rev. Lett.* **79** 4550
[11] Patel A, Protopapas M, Lappas D G and Knight P L 1998 *Phys. Rev.* A **58** R2652
[12] Chism W, Choi D I and Reichl L E 2000 *Phys. Rev.* A **61** 054702
[13] Kwon D H, Chun Y J, Lee H W and Rhee Y 2002 *Phys. Rev.* A **65** 055401
[14] Choi D I and Chism W 2002 *Phys. Rev.* A **66** 025401
[15] Bauer D and Ceccherini F 2002 *Phys. Rev.* A **66** 053411
[16] Gajda M, Piraux B and Rzazewski K 1994 *Phys. Rev.* A **50** 2528
[17] Pont M and Gavrila M 1990 *Phys. Rev. Lett.* **65** 2362
[18] Dörr M, Potvliege R M, Proulx D and Shakeshaft R 1991 *Phys. Rev.* A **43** 3729
[19] Potvliege R M 1998 *Comput. Phys. Commun.* **114** 42
[20] Zakrewski J and Delande D 1995 *J. Phys. B: At. Mol. Opt. Phys.* **28** L667
[21] Muller H G 1999 *Laser Phys.* **9** 138
[22] Muller H G 1999 *Phys. Rev. Lett.* **83** 3158
[23] Kylstra N J, Worthington R A, Patel A, Knight P L, Vázquez de Aldana J R and Roso L 2000 *Phys. Rev. Lett.* **85** 1835
[24] Piraux B and Potvliege R M 1998 *Phys. Rev.* A **57** 5009
[25] Fring A, Kostrykin V and Schrader R 1997 *J. Phys. A: Math. Gen.* **30** 8599